PROPOSAL FOR RESPONSE CONTROL STRUCTURE USING VISCOUS WALL DAMPERS WITH DEFORMATION AMPLIFICATION MECHANISM

R. Tobari[(1)], M. Ishii[(2)], T. Sato[(3)], H. Kitamura[(4)], K. Yoshie[(5)], M. Miyazaki[(6)], K.Sasaki[(7)] and Y. Iwasaki[(8)]

[(1)] *Senior Staff, JFE Civil Engineering and Construction Corp., tobari-ryouta@jfe-civil.com*
[(2)] *Engineering Director, Dr. Eng., Nikken Sekkei Ltd, ishiim@nikken.jp*
[(3)] *Associate Professor, Dr. Eng., Kyushu University, sato@arch.kyushu-u.ac.jp*
[(4)] *Vice President, Dr. Eng, Tokyo University of Science, kita-h@rs.noda.tus.ac.jp*
[(5)] *Engineering Director, Dr. Eng., Nikken Sekkei Ltd, yoshie@nikken.jp*
[(6)] *Manager, Oiles Corporation, m.miyazaki@oiles.co.jp*
[(7)] *General Staff, Dr. Eng., Oiles Corporation, k.sasaki@oiles.co.jp*
[(8)] *General Staff, Oiles Corporation, y.iwasaki@oiles.co.jp*

Abstract

The improvement of the seismic performance of high-rise buildings has become necessary since the 2011 Tohoku Earthquake off the Pacific coast. Response control structures are used extensively to mitigate damage to structural building frames under strong ground motion. A damping force is induced by the deformations acting on the response control devices, and thus, response control structures are affected by both the bending deformation of the entire frame and the frame deformation resulting from the force of the dampers. In the design of high-rise buildings, owing to these deformations, appropriate evaluation of the deformation affecting the response control devices (defined as effective damper deformation) is necessary. In this study, a new structural system with a damper deformation amplification mechanism is proposed to improve the response control performance. In this structural system, the bending deformation of the entire frame, which is usually a factor that reduces the effective damper deformation, increases the effective damper deformation.

The proposed structural system with the effective damper deformation amplification mechanism is illustrated in Figure 1(a). The deformation state of the proposed system within the entire frame is presented in Figure 1(b). The proposed system with wall-type dampers uses forms installed with a beam including two pin joints, and has two characterized deformation amplification effects. Firstly, in the case of a small damper, the direction of the damper deformation caused by the axial deformation of the columns is in the same direction as that of the damper deformation caused by the shear deformation of the main frame. This is a result of the axial force of the column attached to the damper changing from compression to tension, owing to the separation of the main frame. Secondly, the dampers are deformed by the rotation of the beams between two pins geometrically for disposing pins on the inside of the beam. The amplification ratio owing to the geometric deformation is related to the pin position. The deformation state of the proposed system is clarified by the effective damper deformation being separated into components for the shear, bending, and partial deformations of the main frame.

The response control effects of the proposed system were examined using seismic response analysis, with the equivalent period and damping of a 30-story building. The advantage of the proposed system is that seismic responses can be significantly reduced with minimal damping owing to the strong damping effect produced. Moreover, the shear forces are reduced when using the proposed system, particularly by extending the period via stiffness reductions.

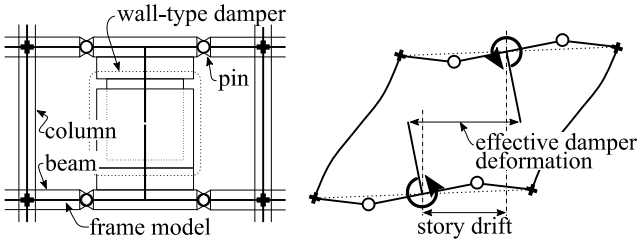

(a) Proposed system (b) Deformation state

Figure 1 Diagram of the proposed system

Keywords: response control structure, effective damper deformation, high-rise building, steel structure, viscous wall damper

1. Introduction

This research proposes a new damping system that can achieve larger damper deformation than a story drift for viscous wall dampers, and evaluates its performance. In the response control structure, the effective damper deformation acting on the damper may be lower than the story drift owing to the deformation of the damper mounting member and surrounding frame, as well as the bending deformation of the entire frame [1] and [2]. During the design of a response control structure, it is important to consider the selection and arrangement of the damper types, so that the effective damper deformation can be sufficiently secured. As represented by the "toggle damping device" [3], an effective damping system has been devised that increases the effective damper deformation of the damper against the story drift [4] and [5]. This is the mechanism that is expected for the amplification effect by geometric deformation. The system proposed in this study differs from the existing technology in that the axial expansion and contraction of the column, which can only reduce the effective damper deformations in the conventional frame, are transformed into an increase in the effective damper deformation.

In this research, the proposed system is applied to a 30-story steel building with viscous wall dampers arranged in multi-story layers, the effective damper deformation components are analyzed, and the deformation state is clarified. In particular, verification is performed by steady-state analysis of the first-order mode and time history response analysis, and the results of the performance evaluation using the equivalent period and damping of the first-order mode are presented. The steady-state analysis of the first-order mode in a response control structure with viscous wall dampers is used as a stress analysis method that is equivalent to static analysis in a response control structure of a displacement-dependent damper.

2. Displacement amplification mechanism applied to viscous wall dampers

As illustrated in the conceptual diagram of Fig. 1, the deformation amplification mechanism applied to the viscous wall dampers proposed in this study uses a pin joint in the middle of the beam, installed on the viscous wall dampers. To explain the concept of deformation amplification, the pin position is set equidistant from the left and right column ends, and horizontal deformation is applied to a one-story, one-span partial frame with rigid columns and beams. Under these assumed conditions, the effective damper deformation of the viscous wall dampers can be expressed by equation (1a), and the ratio γ_1 to the story drift can be expressed by equation (1b) according to the geometric relationship. The relationship between the amplification factor γ_1 and pin position l/L according to equation (1b) is illustrated in Fig. 1(b). In this case, γ_1 increases as l/L increases; that is, as the pin position approaches the beam center.

$$\delta_e = h \cdot \theta \cdot \left(1 + \frac{1}{L/2l - 1}\right),\ \gamma_1 = 1 + \frac{1}{L/2l - 1} \qquad \text{(1a, b)}$$

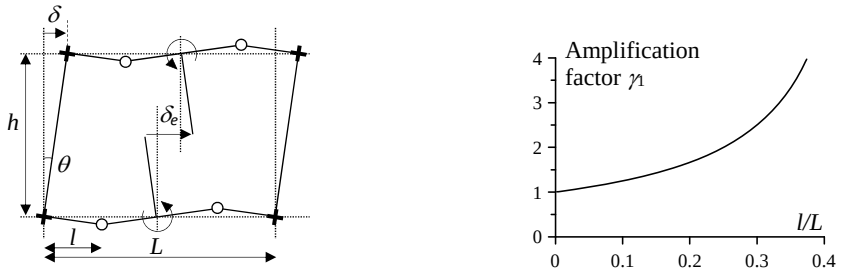

(a) Conceptual diagram of deformation (b) Pin position and amplification factor

Fig. 1 Deformation amplification for horizontal deformation

A mechanism for increasing and decreasing the effective damper deformation when a vertical displacement difference occurs between the left and right columns is described. As indicated in Fig. 2, when the column and beam are rigid, the relationship between the difference between the vertical displacement of

the nodes of the left and right columns, and the effective damper deformation can be expressed by equation (2a). The ratio γ_2 between the effective damper deformation and vertical deformation is expressed by equation (2b). The effective damper deformation increases when the node on the right moves relatively upwards (Fig. 2(a)), and decreases when it moves downwards (Fig. 2(b)). The relationship between the change rate γ_2 and pin position l/L according to equation (2b) is illustrated in Fig. 2(c). As with γ_1, γ_2 increases as the pin position approaches the beam center, which means that, if the effective damper deformation decreases, the decreasing amount also increases.

$$\delta_e = \frac{1}{1-2l/L}\cdot\frac{h}{L}\cdot{}_v\delta\,,\ \gamma_2 = \frac{1}{1-2l/L}\cdot\frac{h}{L} \tag{2a, b}$$

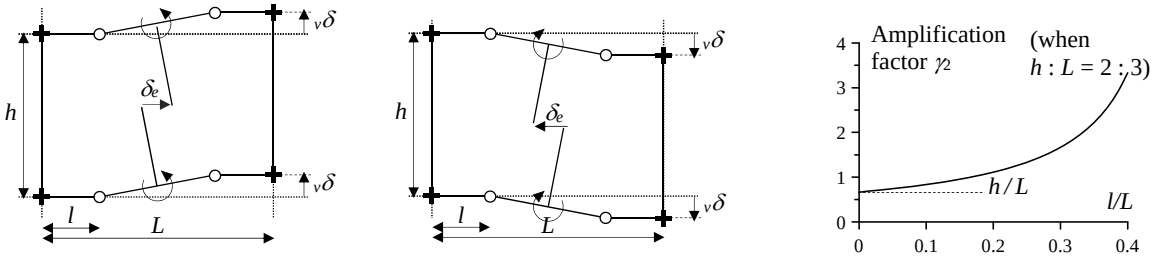

(a) Increasing deformation (b) Decreasing deformation (c) Pin position and amplification factor

Fig. 2 Deformation amplification for vertical deformation

3. Modeling of frame and component separation of effective damper deformation

An outline of the response control structure with viscous wall dampers and a frame model is shown in Fig. 3. This study deals with viscous wall dampers composed of a steel plate and viscous materials. Assuming that the deformation at the center of the upper and lower floors acts uniformly, the rigid region is extended from the central part of the steel plate installed on the beam to half of the floor height. Furthermore, the model connects the ends of the rigid areas in the floor center with dashpots. The beam on which the steel plate is installed is provided with a rigid zone approximately the width of the steel plate. The stiffness of the frame, including the beam–column joint panel, is expressed by setting an equivalent rigid region at the ends of the columns and beams. The axial deformation of the beam is neglected based on the assumption of a rigid floor. The out-of-plane deformation of the viscous wall dampers is not evaluated in this study.

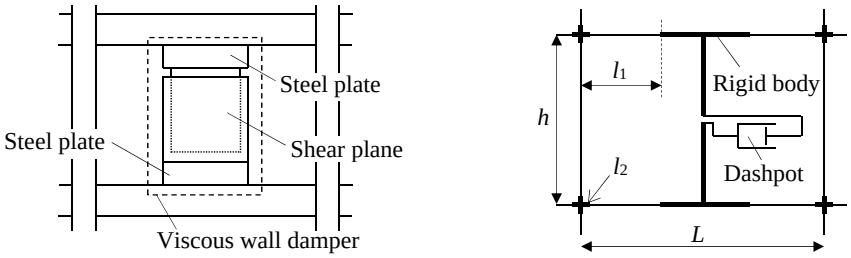

(a) Damper installation diagram (b) Frame model

Fig. 3 Response control structure considered in this study

Next, a method for separating the components of the effective damper deformation using the abovementioned model is described. In this study, the effective damper deformation is defined as the deformation of the dashpot connected to the end of the rigid area at the floor center. In Fig. 4, the component separation of the effective damper deformation is schematically presented. In the figure, δ indicates the story drift, with subscripts indicating each component of the effective damper deformation, and θ indicates the rotation angle. The subscripts are *s*: shear component, *b*: entire bending component, *g*: beam deformation

component, and θ: total rotation of the node, where 1 is the value at the upper part of the viscous wall dampers and 2 is the value at the lower part. As illustrated in Fig. 4, the effective damper deformation of the viscous wall dampers can be expressed by the following equation:

$$\delta_e = \delta_s + \delta_g \,. \tag{3}$$

Equation (3) can be rewritten as the following formula, which defines the difference between the story drift and shear deformation as the bending deformation of the entire frame.

$$\delta_e = \delta - \delta_b + \delta_g \tag{4}$$

As indicated in the above equation, the effective damper deformation is divided into three terms: the story drift, bending deformation of the entire frame, and beam deformation. In this case, δ_b is obtained by equation (5a) using the rigid rotation angle θ_b owing to the bending deformation of the entire frame, while θ_{b1} and θ_{b2} can be calculated by the following equation, using the vertical displacements v_{11}, v_{12}, v_{21}, and v_{22} of the beam end nodes, along with the span length L.

$$\delta_b = \frac{h}{2}\cdot\left(\theta_{b1} + \theta_{b2}\right),\ \theta_{b1} = \frac{v_{11} - v_{12}}{L}\,,\ \theta_{b2} = \frac{v_{21} - v_{22}}{L} \tag{5a, b, c}$$

Further, δ_g can be obtained by the following equation, using the rotation angles θ_1 and θ_2 of the node connected to the viscous wall dampers.

$$\delta_g = \delta_b - \delta_\theta\,,\ \delta_\theta = \frac{h}{2}\cdot\left(\theta_1 + \theta_2\right) \tag{6a, b}$$

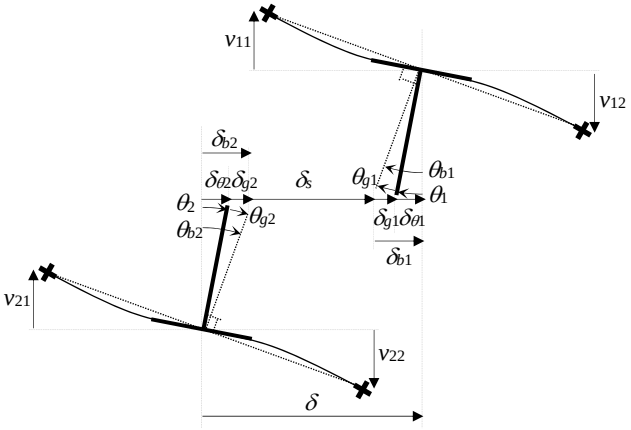

Fig. 4 Decomposition of effective damper deformation

4. Overview of model

4.1 Building model

The building model used in this study is a 30-story steel structure, assuming it to be a high-rise building in which the bending deformation of the entire frame is likely to be dominant. The building has a height of 121.5 m. As indicated in the frame diagram of Fig. 5, the floor height is 5.5 m on the first floor, and 4 m on the second floor and higher. The plane is a 32 m × 38.4 m rectangle composed of six spans in the X-direction and three spans in the Y-direction. The column and beam members are determined based on the allowable stress design for the seismic force with the standard story shear force coefficient C_0 = 0.2 (Table 1). The

analysis is performed with a frame model assuming a rigid floor, and targets in the X-direction. To evaluate the rigidity of the frame, including the beam–column joint panel, an equivalent rigid region is set at the ends of the columns and beams. Time history response analysis is performed using the direct integration method with average acceleration.

4.2 Overview of viscous wall dampers

In the model of the viscous wall dampers, only the nonlinear viscous dashpot is installed, and the deformation of the steel plate is ignored. The beam on which the steel plate is installed is considered as rigid. The viscous wall damper force F_d is expressed by equations (7a, b), and it is proportional to the exponential power of the dashpot speed, where D is the shear gap (= 0.004 m) of the viscous wall dampers.

$$F_d = C_{d1} \cdot \dot{\delta}_d \,,\ |\dot{\delta}_d| / D < 1 \tag{7a}$$

$$F_d = C_{d2} \cdot \dot{\delta}_d{}^{0.59} \,,\ 1 \leq |\dot{\delta}_d| / D \tag{7b}$$

The additional viscous damping amount C_{di} of the i-th layer is determined by the following equation, using the additional viscous damping constant h_d as a parameter. The distribution of C_{di} is a six-step distribution for every five layers.

$$C_{di} = \frac{2h_d}{\omega_{f1}} \cdot K_{fi} \,, \tag{8}$$

where C_{di} is adopted as the primary viscosity coefficient, ω_{f1} is the primary natural frequency of the main frame, and K_{fi} is the horizontal stiffness of the main frame in the i-th layer.

4.3 Outline of response control model using deformation amplification mechanism

The proposed deformation amplification mechanism is applied to a 30-story steel structure building, as described in section 4.1, and pins are provided at two locations on the beam other than the foundation beam at the damper installation position (DA model: deformation amplification model). The pin position l is 1600 mm, the ratio l/L to the span length is 1/4, and the amplification factor owing to horizontal deformation is 2. As illustrated in Fig. 6, the number of dampers per layer is four (notation: 4-unit) or eight (notation: 8-unit). In the proposed model, the beam between the two pins is made rigid in consideration of the effects of installing the viscous wall dampers. A response control model of a conventional frame with dampers arranged in the same positions (CF model: conventional frame model) is used for comparison.

The layer stiffness of the DA model is illustrated in Fig. 7. Compared to the CF model, the layer stiffness of the DA model is reduced by an average of 30% for the 4-unit model and 59% for the 8-unit model. The

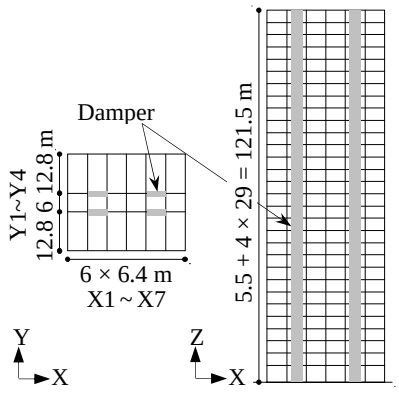

Fig. 5 Building model

Table 1. Member

Inner column
□−600 × 600 × 22 ~ □−600 × 600 × 50
Outer column
□−550 × 550 × 22 ~ □−550 × 550 × 50
Beam
H−600 ×200×12×19 ~ H−600×250×12×25

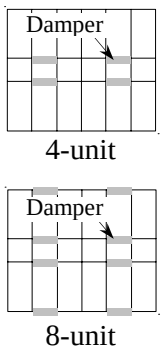

Fig. 6 Damper arrangement

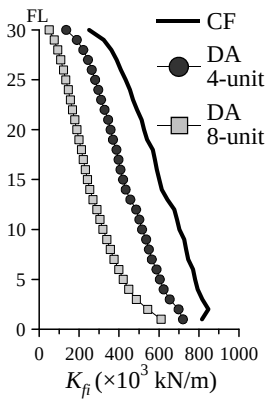

Fig. 7 Story stiffness

primary natural period T_{f1} of the main frame is 4.99 s for the 4-unit model and 6.39 s for the 8-unit model, compared to 4.28 s for the CF model. The viscosity coefficient of the viscous wall dampers in the DA model is determined by equation (8), using the main frame stiffness and primary natural frequency after applying the deformation amplification mechanism.

5. Evaluation of deformation state in steady state of primary mode

Using the decomposition of the effective damper deformation, as described in Section 3, the amplification effect of the effective damper deformation in the DA model is verified. The effective damper deformation components and a conceptual diagram of the deformation state of the main frame for each h_d of the CF and DA models are illustrated in Fig. 8. The solid line is the sum of δ_i, δ_{gi}, and δ_{bi}. The effective damper

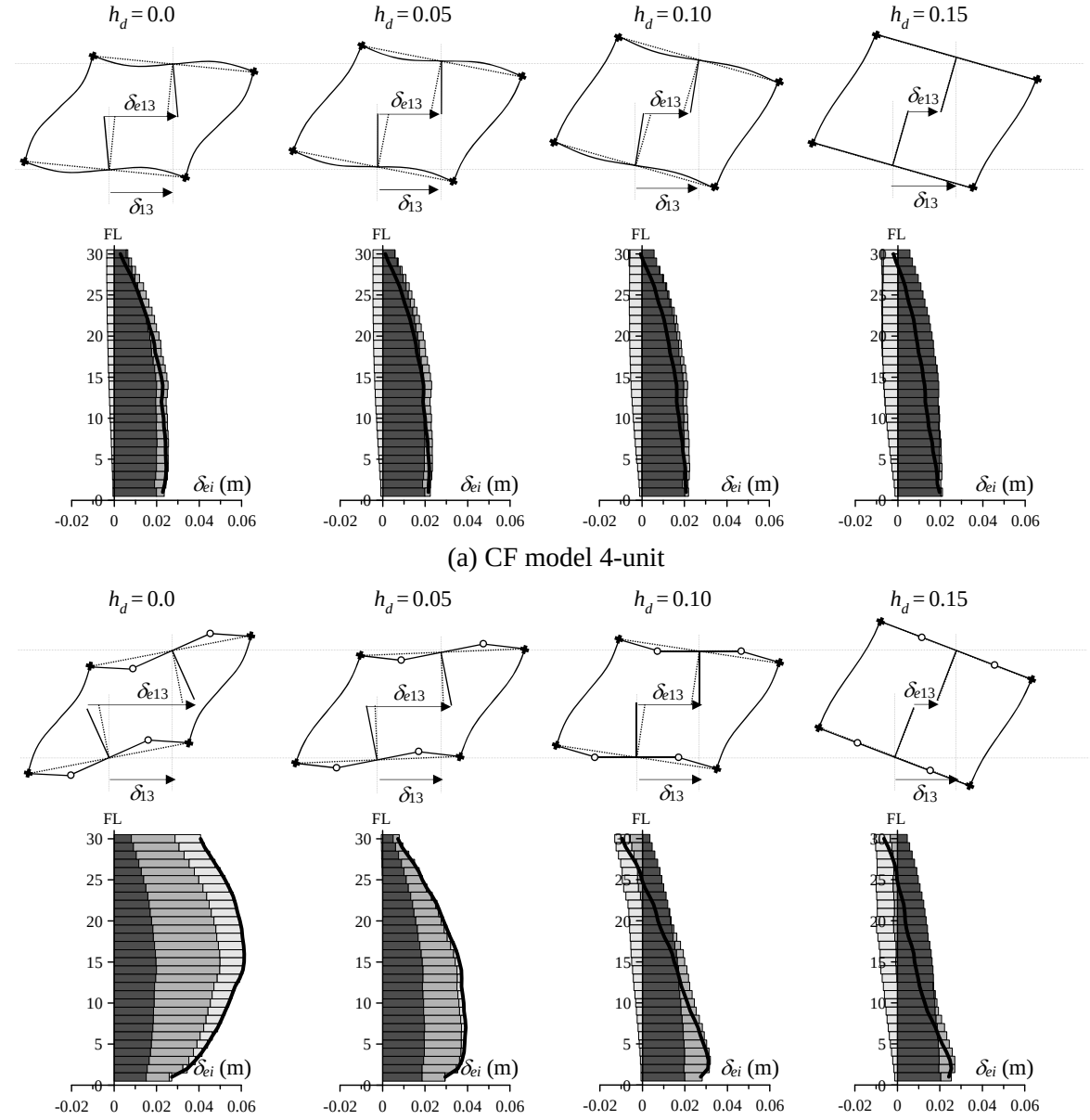

(a) CF model 4-unit

(b) DA model 8-unit

δ_i (story drift angle) δ_{gi} (beam deformation) δ_{bi} (bending deformation of entire frame) δ_{ei} (total)

Fig. 8 Effective damper deformation components and conceptual diagram of frame deformation

deformation components in Fig. 8 provide a sine wave of the primary natural period T_{f1} of the main frame only, and the result when a maximum story drift angle occurs in the steady state is illustrated. The amplitude of the sine wave is adjusted in each analysis case so that the maximum story drift angle is 1/200. In the following, we focus on the results of 13 layers as representative layers.

The effective damper deformation components at h_d = 0.0 in the CF model are increased by the beam deformation and decreased by the bending deformation of the entire frame, and the total value increases by 14% compared to the story deformation. However, the effective damper deformation components of the DA model are increased significantly by the beam deformation and bending deformation of the entire frame, and the total value is 200% higher than the story deformation. As indicated in the frame deformation diagram at h_d = 0.0, the DA model makes it easier for the beam to be deformed than in the DF model, owing to the pin in the middle of the beam. Moreover, the member axis of the beam rotates in reverse compared to the CF model as a result of the bending deformation of the entire frame. Therefore, the main frame is deformed in the direction in which the effective damper deformation increases. Thus, in the DA model, a frame that can receive large effective damper deformation is formed.

In both the DA and CF models, when h_d is large, the beam deformation components and bending deformation of the entire frame component are reduced. As a result, the effective damper deformation decreases when h_d = 0.10 or more. This factor is evident from the frame deformation when h_d is large in Fig. 8(b). This is because the reverse bending of the beam, and axial expansion and contraction of the column owing to the damping force of the viscous wall dampers, work in the same direction to reduce the effective damper deformation, as in the CF model. In the proposed system, with a large h_d, the decrease in the effective damper deformation is remarkable, because a large damping force is generated even with a smaller h_d owing to the effect of amplifying the effective damper deformation.

The effective damper deformation components of the 8-unit model in the CF and DA models are illustrated in Fig. 9. Compared to the effective damper deformation components of the 4-unit DA model in Fig. 8(b), the bending deformation of the entire frame component of the 8-unit DA model is larger. This is because the pins provided at Y1 to Y4 separate the main frame into multi-story rigid frames, with one span on the left and right and two spans at the center, making it easy for the columns to expand and contract. By dispersing the dampers across eight units, the axial expansion and contraction of the columns owing to the damping force of the viscous wall dampers is reduced. This is the same as the case in the CF model.

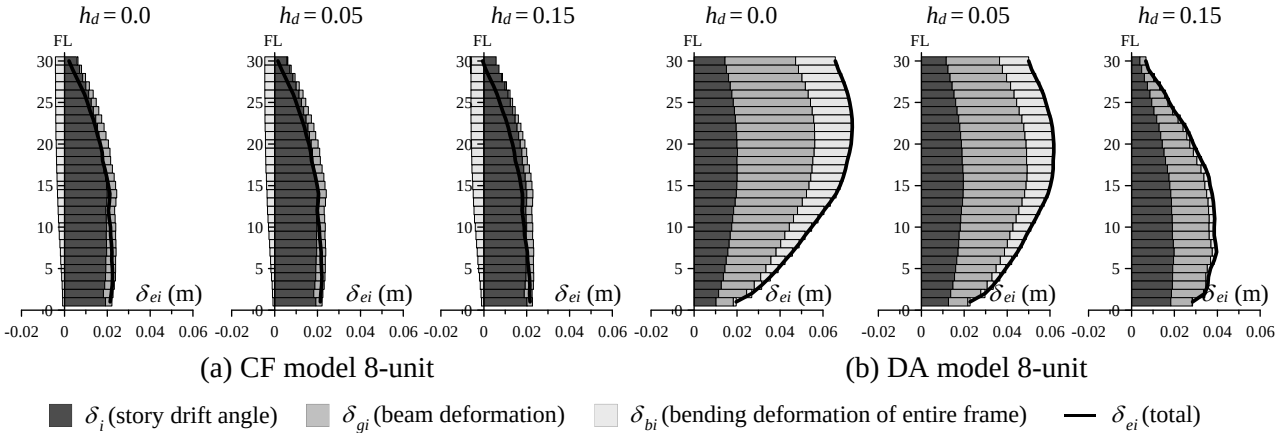

Fig. 9 Effective damper deformation components in 8-unit model

6. Performance evaluation of building using proposed system

6.1 Ground motion

In this study, three artificial ground motions are used. The pseudo-velocity response spectrum S_{pv} = 0.8 m/s (h = 5%) is set as the target response spectrum. The phase characteristics are the EW component of

Hachinohe (1968 Tokachi-oki earthquake), NS component of JMA-KOBE (the 1995 Southern Hyogo Prefecture Earthquake), and NS component of El Centro (1940 Imperial Valley earthquake), which are hereafter referred to as Hachinohe, Kobe, and El Centro, respectively. The acceleration time history waveform of the ground motion and pseudo-velocity response spectrum, together with the target response spectrum are illustrated in Fig. 10.

6.2 Performance evaluation by time history response analysis

A comparison of the maximum story drift angle R, response acceleration A, story shear force Q, and effective damper deformation ratio α_e between the CF and DA models when h_d = 0.05 to 0.30 is illustrated in Fig. 11.

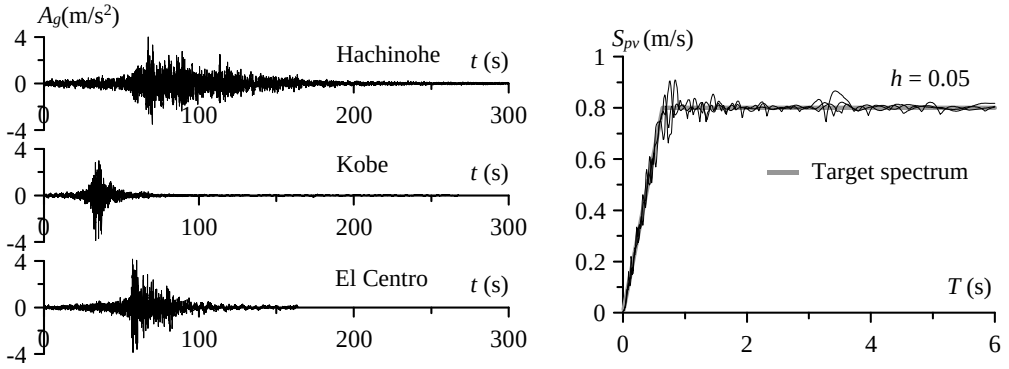

Fig. 10 Acceleration waveform and pseudo-velocity response spectrum of ground motion

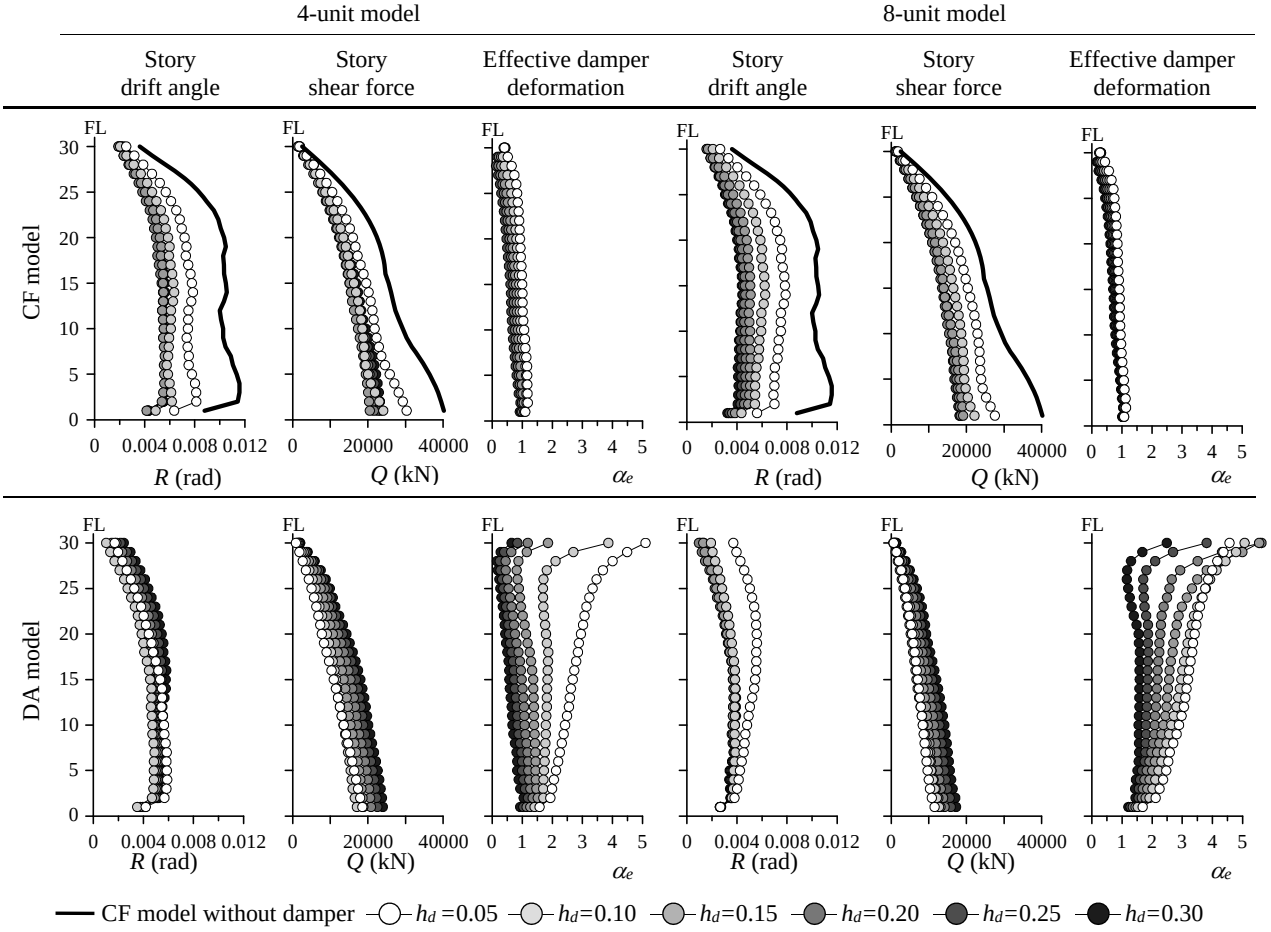

Fig. 11 Comparison of time history response analysis results between DA and CF models

The ground motion is Hachinohe, and the response of the CF model without dampers is indicated by a solid line for comparison. In Fig. 11, comparing the response of the DA model with that of the CF model demonstrates that the story drift angle is reduced more than or equal to the same arrangement in the CF model, while the story shear force is significantly reduced. The decrease in the story shear force is owing to the effect of the longer period and increasing equivalent damping, as described in detail in the following section. The story drift angle and story shear force of the DA model tend to reach an extreme value when h_d is smaller than that of the CF model, as demonstrated in the examination of the first-order mode in the steady state in Section 5.

6.3 Performance evaluation by equivalent damping h_{eq} and equivalent period T_{eq}

In the DA model, the input level on the response spectrum fluctuates because the period becomes longer owing to the decrease in the stiffness of the main frame. In this section, the response reduction effect is verified based on the equivalent damping h_{eq} and equivalent period T_{eq}.

6.3.1 Calculation of h_{eq} and T_{eq}

The calculation method for h_{eq} and T_{eq} is presented below, but the detailed explanation is omitted. A series of details of the calculation method can be found in [7]. Firstly, according to the methods described in [8] and [9], the frame characteristic values and pseudo-brace stiffness are calculated, and a shear spring model that is capable of evaluating the damper deformation appropriately is created. Next, the equivalent damping h_{eqsi} of each layer is evaluated based on the equivalent linearization method of a system with a nonlinear viscous damper, as described in [10] and [11]. Finally, the equivalent damping h_{eqsi} of each layer is weighted by the elastic strain energy W_{esi}, and the overall equivalent damping h_{eqs} is evaluated by the following equation.

$$h_{eqs} = \sum_{i=1}^{N} h_{eqsi} \cdot W_{esi} \Big/ \sum_{i=1}^{N} W_{esi} \tag{9}$$

The natural period T_{eqs} of the equivalent one-mass system, considering the equivalent stiffness of the damper, can be obtained by the following formula [12]:

$$T_{eqs} = 2\pi \sqrt{\sum_{i=1}^{N} \left(m_i \sum_{j=1}^{i} \frac{B_{sj}}{K_{eqsj}} \right)}, \tag{10}$$

where m_i is the mass of each layer, B_{si} is the ratio of the shear force of each layer Q_{si} to the base layer shear force Q_{Bs}, and K_{eqsi} is the equivalent stiffness of each layer.

6.3.2 Calculation results of h_{eq} and T_{eq}

The values of h_d and T_{eqs} when h_{eqs} is maximized are displayed in Table 2. The response changes on the response spectrum of the artificial wave owing to the fluctuations in the h_{eqs} and the T_{eqs} at h_d in Table 2 are illustrated in Fig. 12. In this case, T_f is the natural period of only the main frame of the CF model, while T_{fd} is the natural period of only the main frame of the DA model. The response spectrum of the artificial wave indicated in Fig. 10 is obtained by the velocity response spectrum in section 6.1 by determining the damping effect coefficient D_h [13] and converting it into a pseudo-acceleration response and pseudo-displacement response. The broken arrow of B in the figure indicates the change in the spectrum value owing to the fluctuation of the equivalent period. The broken arrow of C indicates the change in the spectrum value owing to an increase in the equivalent damping. Furthermore, the broken arrow of A indicates the change in the spectrum value owing to a periodic change resulting from the pin attached to the frame in the DA model.

As indicated in the figure, in the CF model, the displacement is reduced and the acceleration is increased by shortening the period (effect B), while the displacement and acceleration are reduced by the increased damping (effect C). However, in the DA model, the period becomes longer owing to the decrease in the frame stiffness, and effect A of the acceleration reduction and displacement increase is added. As a result, the acceleration reduction effect is larger than that in the CF model, and the displacement tends to

increase, exhibiting characteristics similar to the seismic isolation structure. However, unlike the seismic isolation structure, the displacement is not concentrated on a specific layer, but is distributed to each layer, and it is necessary to set the parameters of the main frame and damper of each layer appropriately. In the DA model of Fig. 12, it can be observed that both the acceleration and displacement are reduced substantially owing to the strong damping effect.

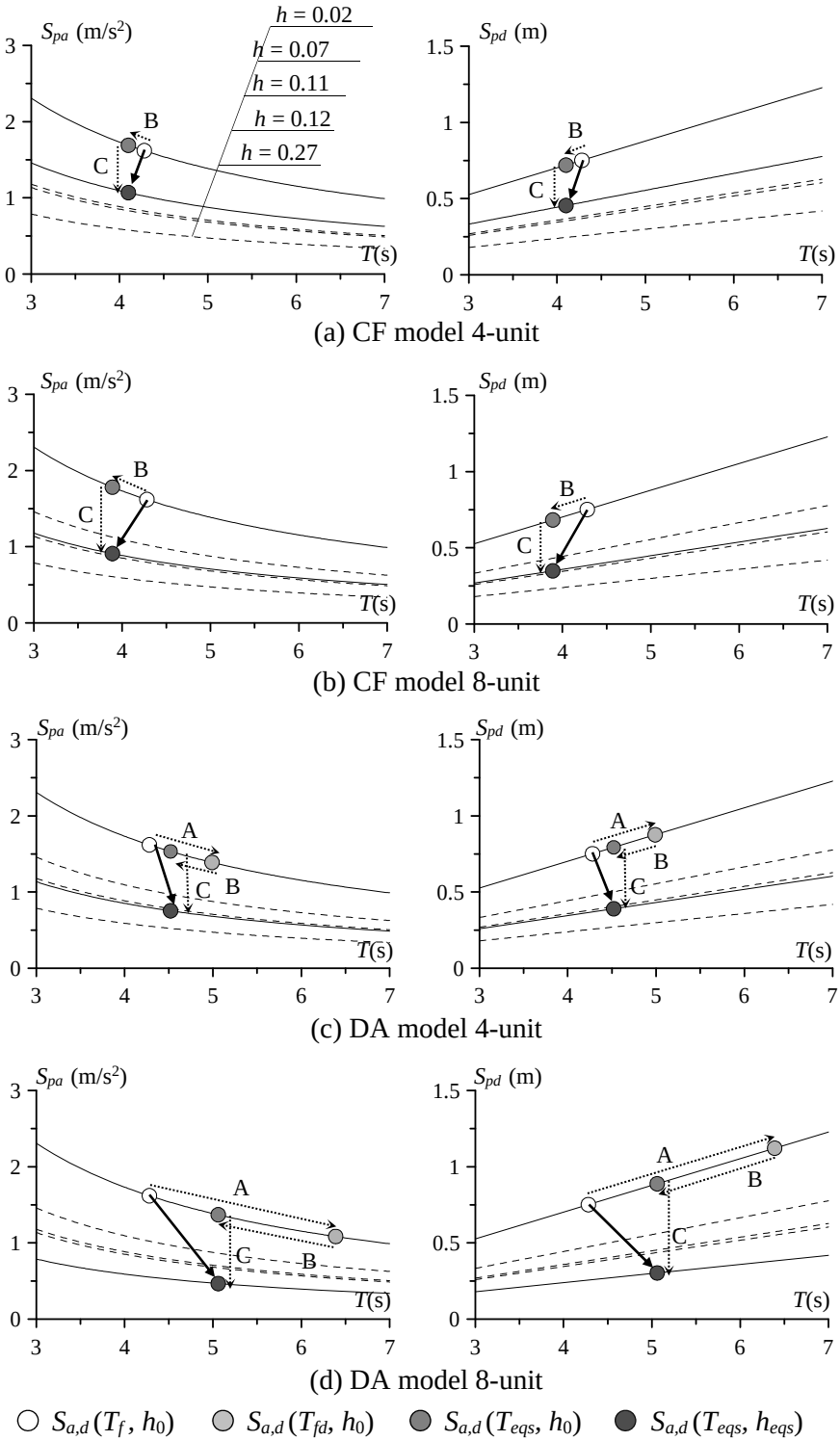

(a) CF model 4-unit

(b) CF model 8-unit

(c) DA model 4-unit

(d) DA model 8-unit

○ $S_{a,d}(T_f, h_0)$ ● $S_{a,d}(T_{fd}, h_0)$ ● $S_{a,d}(T_{eqs}, h_0)$ ● $S_{a,d}(T_{eqs}, h_{eqs})$

Fig. 12 Response changes on response spectrum

7. Conclusions

A new system that can achieve large effective damper deformation has been proposed by providing a pin joint in the middle of the beam on which the viscous wall dampers are installed. Moreover, its effectiveness was examined using a 30-story steel building model. Although the study is limited in its scope, the results obtained are summarized below.

1) The effective damper deformation was represented by three components, and the difference between the deformation state of the conventional system and proposed system was discussed. In the proposed system, when the damper amount was small, both the rotational deformation of the beam and overall bending deformation of the entire frame component contributed significantly to the increase in the effective damper deformation.

2) The effect of reducing the response of the proposed system using the equivalent damping and period was considered. It was clarified that the damping was added after the period increased owing to the decrease in the frame stiffness, and the story shear force was significantly reduced.

References

[1] Kubota M, Ishimaru S, Hata I (2000): Vibration testing for energy absorption performance in steel frame of toggle damping equipment. *2th Japan Seismic Symposium*, 8-9 November, Tokyo, Japan. (in Japanese)

[2] Shinbayashi M, Arakawa G (2005): Dynamic Loading Test of Vibration Control Device with Amplification System. *Summaries of technical papers of annual meeting*, AIJ, pp.443-445. (in Japanese)

[3] Sugimura Y, Nagae K, Saito K, Nakaminami S, Toyota K, Arima F (2002): Dynamic Loading Test and Application to a High-Rise Building of Viscous Damping Devices with Amplification System. *Summaries of technical papers of annual meeting*, AIJ, pp.709-716. (in Japanese)

[4] Furuya K, Soeta K, Sato D, Kitamura H, Ishii M, Yoshie K, Miyazaki M, Sasaki K, Iwasaki Y (2012):Evaluation of the vibration control performance for high-rise elastic frame with hysteretic dampers focusing on effective damper deformation ration. *Journal of Structural Engineering*, AIJ, 58B, pp.197-207. (in Japanese)

[5] Tobari R, Sato D, Furuya K, Kitamura H, Ishii M, Yoshie K, Miyazaki M, Sasaki K, Iwasaki Y (2013):The evaluation of the vibration control performance of the building with hysteretic damper using frame parameters for control. *Journal of Structural Engineering*, AIJ, 59B, pp.321-327. (in Japanese)

[6] JSSI (2013): Manual for Design and Construction of passively-Controlled Buildings (3rd Edition) ,The Japan Society of Seismic Isolation. (in Japanese)

[7] Tobari R, Ishii M, Sato T, Kitamura H, Yoshie K, Miyazaki M, Sasaki K, Iwasaki Y (2014): Proposal for response control structure using viscous wall dampers with deformation amplification mechanism. *Journal of Structural and Construction Engineering*, AIJ, 79(706), pp.1741-1750. (in Japanese)

[8] Ishii M , Kasai K (2010): Shear spring model for time history analysis of multi-story passive controlled buildings. *Journal of Structural and Construction Engineering*, AIJ, 75(647), pp.103-112. (in Japanese)

[9] Kasai K, Iwasaki K (2006): reduced expression for various passive control systems and conversion to shear spring model. *Journal of Structural and Construction Engineering*, AIJ, 71(605), pp.37-46. (in Japanese)

[10] Kasai K, Suzuki A, Oohara K (2003): Equivalent linearization of a passive control system having viscous dampers dependent on fractional power of velocity. *Journal of Structural and Construction Engineering*, AIJ, 68(574), pp.77-84. (in Japanese)

[11] Kasai K, Ogura T, Suzuki A (2007): Passive control design method based on tuning of equivalent stiffness of nonlinear viscous damper. *Journal of Structural and Construction Engineering*, AIJ, 72(618), pp.97-104. (in Japanese)

[12] Shibata A (2003): Dynamic Analysis of Earthquake Resistant Structures, Morikita publishing Co., Ltd. (in Japanese)

[13] Kasai K, Ito H, Watanabe A (2003): Peak response prediction rule for a SDOF elasto-plastic system based on equivalent linearization technique . *Journal of Structural and Construction Engineering*, AIJ, 68(571), pp.53-62. (in Japanese)

